

Received 24 December 2021; accepted 25 February 2022. Date of publication 8 March 2022; date of current version 24 March 2022.  
The review of this article was arranged by Editor Z. Zhang.

Digital Object Identifier 10.1109/JEDS.2022.3157785

# Analog Read Noise and Quantizer Threshold Estimation From Quanta Image Sensor Bit Density

ERIC R. FOSSUM<sup>1</sup> (Fellow, IEEE)

<sup>1</sup>Thayer School of Engineering, Dartmouth College, Hanover, NH 03755, USA

CORRESPONDING AUTHOR: E. R. FOSSUM (e-mail: eric.r.fossum@dartmouth.edu)

This work was supported in part by the Jet Propulsion Laboratory under Grant RSA 1658937; in part by the NASA Award Subcontract from Rochester Institute of Technology under Grant 80NSSC20K0310; and in part by the gift from Goodix Technology Inc., San Diego, CA, USA.

**ABSTRACT** Estimation of the analog read noise level and quantizer threshold level to within a few hundredths of an electron can be obtained by measuring the output bit density,  $D$ , of a single-bit quanta image sensor (1bQIS) as a function of quanta exposure,  $H$ . Analysis of the  $D$ - $H$  characteristics as a function of read noise and quantizer threshold levels is performed and a procedure for extraction of estimated read noise and quantizer threshold is suggested and demonstrated.

**INDEX TERMS** Quanta image sensor, read noise, SPAD image sensor, CMOS image sensor, CIS, QIS.

## I. INTRODUCTION

The Quanta Image Sensor (QIS) is a photon-counting image sensor first proposed in 2005 [1], [2]. The QIS can be implemented either as a single-bit (1b) or multi-bit (mb) device, where the latter permits photon-number resolution [3]. This paper is focused on 1bQIS but most mbQIS devices can be operated as a 1bQIS. The specialized pixel is referred to as a jot. A 1Mjot 1bQIS using CMOS image sensor (CIS) technology with 1.1 $\mu$ m pixel pitch was demonstrated in 2017 [4]. The CIS-QIS operates at room temperature without the use of avalanche multiplication and enables the lower bit-error rate (BER) counting of photoelectrons. A 1Mjot 1bQIS implemented using single-photon avalanche detector (SPAD) technology and 9.4 $\mu$ m pixel was demonstrated in 2020 [5] and a 3.2Mjot, 6.39 $\mu$ m pixel pitch SPAD-mbQIS with an 11b counter per pixel was presented at the end of 2021 [6]. The latter SPAD-QIS pixel is 34x larger than the CIS-QIS pixel to accommodate avalanche photodiodes with high electric fields but low crosstalk and the 11b digital counter in a second layer of a stacked sensor structure. SPADs can generally permit faster photon-arrival-time gating. Generally, most state-of-the-art SPAD-QIS devices tend to have higher dark current or dark count rate (DCR) compared to CIS-QIS, and the photon detection efficiency (PDE) is also lower.

When accurate knowledge of the presence or absence of a photoelectron is needed, especially in scientific imaging

instruments, low read noise is needed to prevent false negatives and false positives; that is, a low BER is desired, and the BER is very dependent on read noise [7]. Measurement of deep sub-electron read noise has traditionally required an analog-readout signal chain [8]. For CIS-QIS and SPAD-QIS, the digital nature of the output precludes direct measurement of the input-referred analog read noise of the image sensor. An ancillary analog channel can be added to the sensor to allow readout of a single jot or an ensemble of jots, but such a pixel may have different noise characteristics compared to a jot used for digital readout due to circuit design, operational sampling and/or operational speed.

In this paper, a methodology is proposed for estimating input-referred analog read noise and quantizer analog threshold voltage level based on the output bit density as a function of light level or quanta exposure. This is particularly useful for CIS-QIS. For SPAD-QIS, measurement of quantizer threshold is typically moot due to avalanche multiplicative gain, and read noise is usually not of concern, although the bit density measured in the dark may be limited by the higher dark count rate (DCR) in a SPAD-QIS rather than by read noise as is the case for CIS-QIS.

Prior to proposing the methodology, analysis of the QIS bit density response is performed to understand the impact of read noise, dark current and quantizer threshold variation.

## II. ANALYSIS OF QIS BIT DENSITY

### A. PHOTON OR PHOTOELECTRON GENERATED BIT DENSITY

Bit density is the number of logic “ones” divided by the total number of bits read out, where a logic one indicates the arrival of at least one photoelectron. It could be for a single jot read out many times (e.g., many frames), or a group of jots read out for one or more frames.

If the average number of collected photoelectrons by a pixel per frame is  $H$ , called the photoelectron quanta exposure, then the probability that  $k$  photoelectrons are collected is given by the Poisson distribution probability mass function  $\mathbb{P}[k]$  according to:

$$\mathbb{P}[H, k] = \frac{e^{-H} H^k}{k!} \quad (1)$$

Ideally, the bit density is just [3]:

$$D = 1 - e^{-H} \quad (2)$$

where  $D \cong H$  for  $H \ll 1$ .

When corrupting readout noise and a quantizer is included, the expected bit density is more complicated. As shown in [7] the readout-voltage probability-density function (ROVPDF),  $P[U]$ , can be written as:

$$P[U] = \sum_{k=0}^{\infty} \frac{\mathbb{P}[H, k]}{\sqrt{2\pi} u_n^2} \exp\left[-\frac{(U-k)^2}{2u_n^2}\right] \quad (3)$$

where  $U$  is the readout voltage normalized by the conversion gain (CG) with units of electrons, and  $u_n$  is the similarly normalized read noise with units of electrons r.m.s.

In a 1bQIS, with a quantizer threshold set at  $U_T$ , the bit density  $D$  is given by:

$$D = \int_{U_T}^{\infty} P[U] dU \quad (4)$$

which yields  $D$  as a function of photoelectron quanta exposure  $H$ , quantizer threshold  $U_T$ , and input-referred analog read noise  $u_n$  in (4).

$$D = \frac{1}{2} \sum_{k=0}^{\infty} \mathbb{P}[H, k] \operatorname{erfc}\left[\frac{U_T - k}{\sqrt{2} u_n}\right] \quad (5)$$

As illustrated in Fig. 1, the bit density,  $D$ , corresponds to the integral under the red  $P[U]$  curve from  $U = U_T$  to  $\infty$ . The read noise is chosen to illustrate how the various components contribute, but for low BER, the read noise is targeted to be 0.15e- r.m.s. or less [3].

### B. BIT DENSITY IN THE DARK

In the dark, where the photoelectron quanta exposure  $H=0$ , all but the  $k=0$  component of Fig. 1 disappear, and the bit density is limited by either the tail of the ROVPDF crossing the quantizer threshold or by thermally generated dark current or dark counts. (Other processes can also result in dark current especially when high electric fields are involved.)

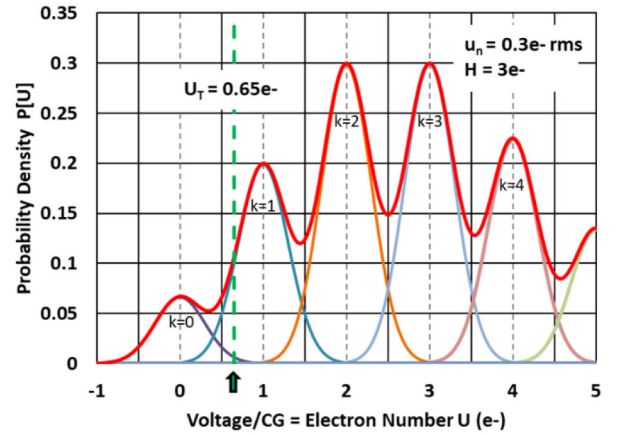


**FIGURE 1.** ROVPDF  $P[U]$  shown in red for a jot with quanta exposure  $H=3.0e^-$ , and read noise  $u_n$  of  $0.3e^-$ -rms. The dashed green line shows a quantizer threshold  $U_T$  of  $0.65e^-$ . The normal distribution components for  $k=0,1,2,3,4$  of  $P[U]$  are shown in the other colors.

In the first case, the Poisson distribution probability mass function  $\mathbb{P}[H, k] = 1$  for  $k = 0$ , and 0 for  $k > 0$ , so the dark bit density  $D_{dark}$  becomes, in the absence of dark current,

$$D_{dark} = \frac{1}{2} \operatorname{erfc}\left[\frac{U_T}{\sqrt{2} u_n}\right] \quad (6)$$

In the second case, thermally generated dark current, or dark count rate with average arrival rate  $H_{dark}$ , increases the dark bit density to (assuming dark-electron arrivals are well-described by Poisson statistics):

$$D_{dark} = \frac{1}{2} \sum_{k=0}^{\infty} \mathbb{P}[H_{dark}, k] \operatorname{erfc}\left[\frac{U_T - k}{\sqrt{2} u_n}\right] \quad (7)$$

More generally, the bit density can be written as:

$$D = \frac{1}{2} \sum_{k=0}^{\infty} \mathbb{P}[H + H_{dark}, k] \operatorname{erfc}\left[\frac{U_T - k}{\sqrt{2} u_n}\right] \quad (8)$$

where the photoelectron and dark electron average arrival rates are explicitly shown. If the number of pixels readout is  $M$ , all with quanta exposure  $H$ , the standard deviation  $\sigma_1$  in the number of photoelectrons detected, a.k.a. noise, is given in [3] as:

$$\sigma_1 = \sqrt{M \cdot D(1 - D)} \quad (9)$$

### C. EFFECT OF READ NOISE ON BIT DENSITY VS. QUANTA EXPOSURE

The effect of read noise on bit density vs. quanta exposure for a nominal quantizer threshold, no dark current, and various read noise levels is shown in Fig. 2 on a log-log scale. It can be seen that the read noise has little effect on bit density for  $H > 1e^-$ , and for  $H < 1e^-$ , read noise limits the reduction in bit density for lower quanta exposure. For read noise of 0.15e- r.m.s., the bit density shows deviation from linearity by  $H < 0.001e^-$ , or an average of one photoelectron arrival per 1000 readouts. The results are consistent with [7, Fig. 6].

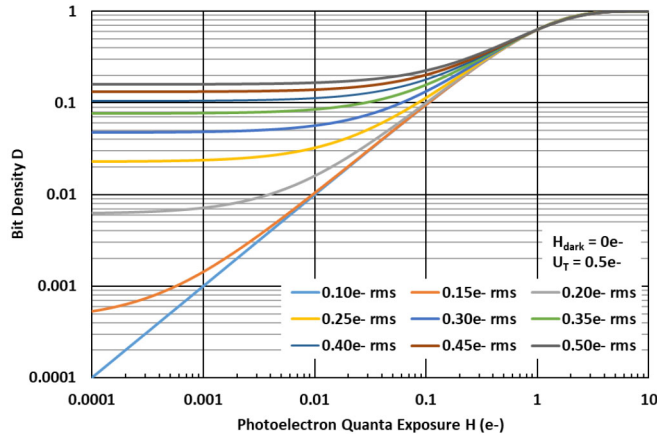


**FIGURE 2.** Bit density  $D$  as a function of photoelectron quanta exposure  $H$  for  $H_{\text{dark}} = 0e^-$  and quantizer threshold  $U_T = 0.5e^-$  and various read noise  $u_n$  levels.

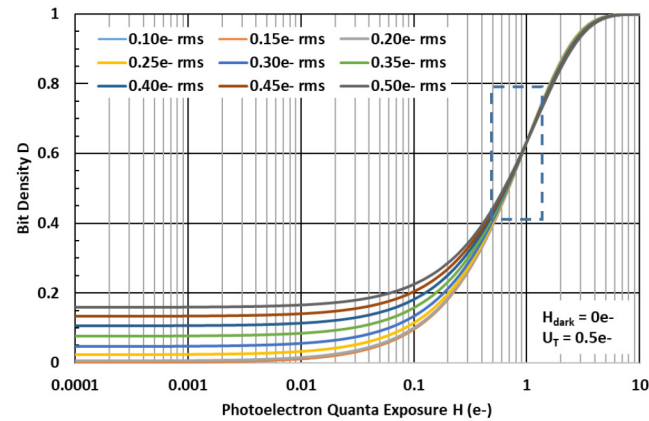


**FIGURE 3.**  $D - \log H$  version of Fig 2. The dashed line box indicates the "throat" region of interest.

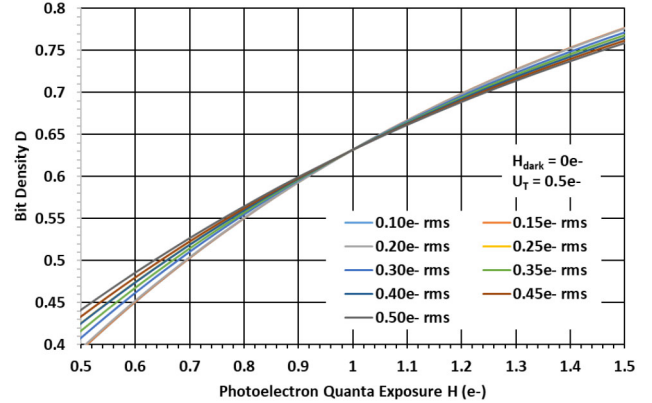
The  $D-H$  characteristic and corresponding noise  $\sigma_1$  was first experimentally verified using a SPAD QIS [9].

Fig. 3 is a  $D - \log H$  version of Fig. 2 to illustrate how read noise elevates the low-light (left or "tail" side) of the response curve. A region of interest, referred to as the "throat," around  $H=1$  (shown by dashed lines) is expanded in Fig. 4.

#### **D. BIT DENSITY INSENSITIVITY TO READ NOISE AT UNITY QUANTA EXPOSURE**

As shown in Fig. 4, at  $H = 1$  with  $H_{\text{dark}} = 0$  and  $U_T = 0.5e^-$ , the bit density is relatively insensitive to read noise and has approximate value  $D = 1 - e^{-1}$  for  $u_n \lesssim 0.5e^-$  r.m.s. For non-zero  $H_{\text{dark}}$ , the position of insensitivity just shifts to  $H = 1 - H_{\text{dark}}$ .

This interesting insensitivity has been proven mathematically by Chan [10] after a discussion of this paper, but for this paper an intuitively satisfying explanation is presented, as illustrated in Fig. 5. Referring to Fig. 5, which shows  $P[U]$  and its  $k=0,1,2,3,4$  components, it is seen that the  $k=0$  component (purple curve) is of equal amplitude and



**FIGURE 4.** Fig. 3's region of interest plotted as  $D$  vs.  $H$ .

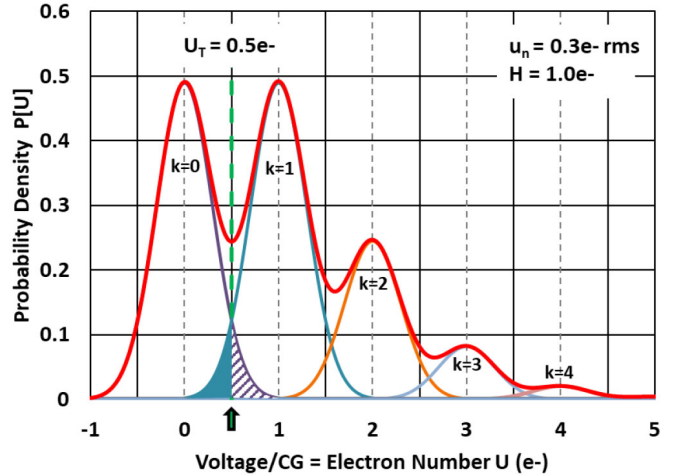


**FIGURE 5.** ROVPDF  $P[U]$  shown in red for a jot with quanta exposure  $H=1.0e^-$  and read noise  $u_n$  of  $0.3e^-$  rms. The dashed green line shows a quantizer threshold  $U_T$  of  $0.5e^-$ . The normal distribution components for  $k=0,1,2,3,4$  of  $P[U]$  are shown in the other colors.

width as the  $k=1$  component (blue curve) of  $P[U]$ , since  $H=1$ , thus making  $\mathbb{P}[0] = \mathbb{P}[1]$ . Recalling that:

$$D = \int_{U_T}^{\infty} P[U] dU = 1 - \int_{-\infty}^{U_T} P[U] dU \quad (10)$$

and looking at the integral of the  $P[U]$  curve for  $U < U_T$ , (equal to  $1-D$ ) it is readily apparent that the integral lost from the  $k=0$  component for  $U > U_T$  is equal to the integral gained from the  $k=1$  component for  $U < U_T$  (see shaded areas). Further, it is apparent that if  $u_n \lesssim 0.5e^-$  r.m.s., the integral of the  $k > 1$  components contributes negligibly to  $1-D$ . In essence, the integral of the  $k=0$  component is  $\mathbb{P}[0]$  and is equal to  $1-D$ , and thus:

$$D = 1 - \mathbb{P}[0] = 1 - e^{-1} \quad (11)$$

which is insensitive to read noise  $u_n$ , if  $u_n \lesssim 0.5e^-$  r.m.s.

#### **E. EFFECT OF DARK CURRENT ON BIT DENSITY VS. QUANTA EXPOSURE**

Dark current in CIS-QIS is typically about  $0.1e^-/\text{sec}/\text{pixel}$  at room temperature [4]. At 1kfps operation this leads to

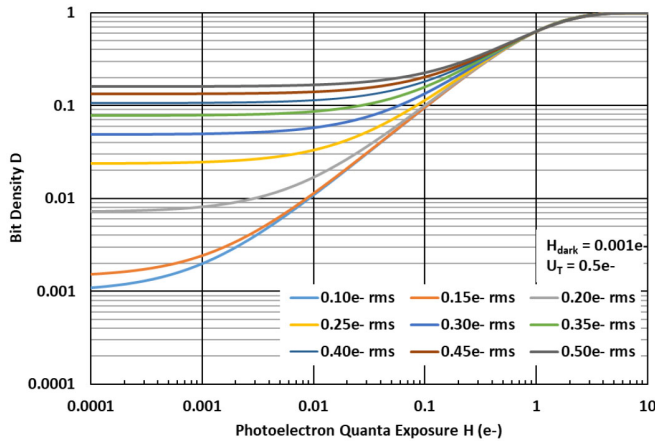


**FIGURE 6.** Bit density  $D$  as a function of photoelectron quanta exposure  $H$  for  $H_{dark} = 0.001e^-$  and quantizer threshold  $U_T = 0.5e^-$  and various read noise  $u_n$  levels.

an expected value of  $H_{dark}$  of  $0.0001e^-$ . For the SPAD-QIS [5], with a dark count rate of  $2e^-/sec/pixel$  at  $24kfps$ , the expected value of  $H_{dark}$  is about the same. Of course, these are just average or median values and there will be outliers. Operating temperatures can also impact  $H_{dark}$  values. The main effect of dark current is to limit the minimum achievable bit density.

As an example, in Fig. 6 the effect of  $H_{dark} = 0.001e^-$  on the  $\log D - \log H$  characteristics is shown as a function of read noise. Compared to Fig. 2, the largest impact is on the lowest read noise curves, pushing them up in bit density as limited by  $H_{dark}$ . There is also little impact for  $H \gtrsim 10 H_{dark}$ . When the same curves are plotted on  $D - \log H$ , there is little effect of the dark current observable due to the change in bit density scale.

### F. EFFECT OF QUANTIZER THRESHOLD ON BIT DENSITY VS. QUANTA EXPOSURE

The effect of quantizer threshold on bit density as a function of quanta exposure with fixed read noise of  $0.15e^-$  r.m.s. is shown in Fig. 7 in a  $\log D - \log H$  plot. The nominal threshold is  $0.5e^-$  (red dashed curve). Reducing the threshold increases the chance of a false positive, and likewise increasing the threshold increases the chance of a false negative. Further increasing the threshold  $U_T$  to  $\gtrsim 1.25e^-$  causes the transfer curve to rapidly shift from linear behavior to quadratic behavior and have  $2x$  the slope on the  $\log D - \log H$  plot. Further increases in threshold cause similar jumps in slope (not shown). It is interesting that increasing the threshold from  $0.5e^-$  to  $0.7e^-$  straightens the transfer curve at low light levels and seems to mitigate the effect of read noise on linearity at very low light levels. Unfortunately this effect is dependent on the read noise level and is not recommended.

In Fig. 8, the data in Fig. 7 is replotted on a  $D - \log H$  plot to show the effect of quantizer threshold on “throat” width.

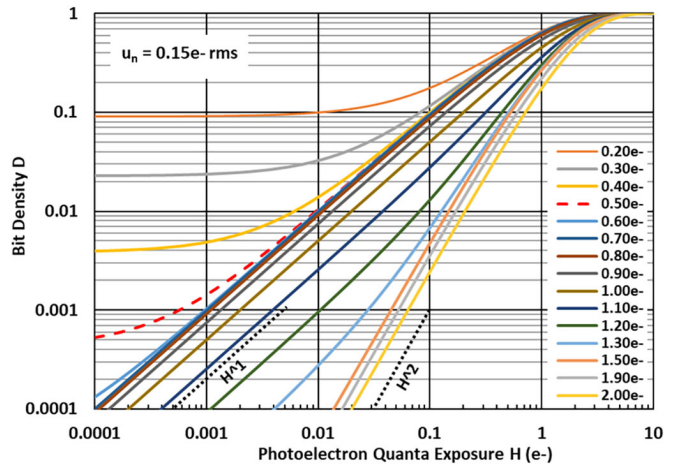


**FIGURE 7.** Bit density  $D$  as a function of photoelectron quanta exposure  $H$  for  $u_n = 0.15e^-$  r.m.s. for various quantizer thresholds  $U_T$ . Linear and quadratic slopes are drawn with dotted lines for reference.

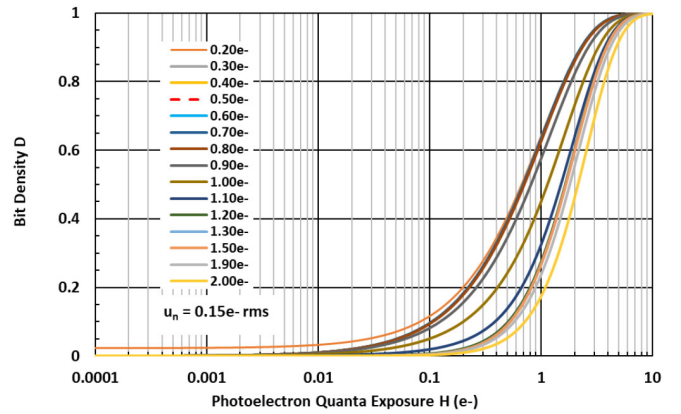


**FIGURE 8.** Fig. 7 replotted on a  $D - \log H$  scale to show the effect of quantizer threshold on “throat” thickness in the region where  $H=1$ .

### G. SUMMARY OF ANALYSIS

The effects of read noise, dark current, and quantizer threshold on the bit density output by a 1bQIS have been analyzed.

- 1) The main effect of increasing read noise is to “fan” the tail section of the  $D - \log H$  curve and erroneously elevate the low light response, preventing the QIS from producing the low bit density representative of low light quanta exposures. The throat part of the curve is mostly insensitive to read noise.
- 2) The effect of dark current is to elevate the tail section of the curve so that  $D_{dark} = H_{dark}$ , which can be further elevated by read noise. Dark current has little effect on the throat section of the  $D - \log H$  response curve.
- 3) The main effect of increasing quantizer threshold variation is to shift the “throat” of the curve mostly to the right. Quantizer threshold variation has little effect on the tail section of the  $D - \log H$  response curve except for very low thresholds.



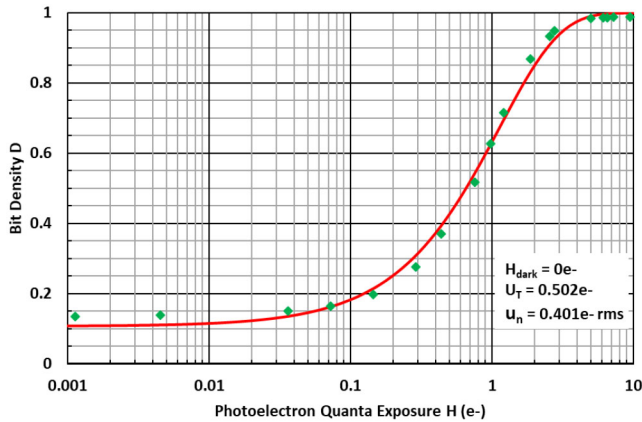


**FIGURE 9.** Experimental 1bQIS binary data plotted on  $D - \log H$  (green diamonds) and least-squares fit (red line) using  $U_T = 0.502e^-$  and  $u_n = 0.401e^-$  r.m.s.

### III. METHODOLOGY TO ESTIMATE READ NOISE AND QUANTIZER THRESHOLD

In the characterization of binary-output 1bQIS devices, experience has shown that estimation of read noise and quantizer threshold has been a challenge. In [4] it was found that the measured  $D - \log H$  characteristic of some jots gave results consistent with theory, and other jots had different characteristics. Ultimately it was decided that there was significant variation in the quantizer threshold from jot to jot and read noise was estimated from separate analog outputs. But, the input-referred read noise for the binary-output channels remained unknowable from direct measurement.

When characterizing 1bQIS, the first concern is calibrating the light source for  $H$ . (Perhaps in the future a QIS-based light meter can be used!) If the read noise is low ( $< 0.5e^-$  rms), and the threshold is well-controlled in the  $0.2e^-$  to  $0.8e^-$  range ( $0.5e^- \pm 0.3e^-$ ) then the bit density from the QIS should be about 0.63 when  $H = 1$ . If the quantizer threshold is adjustable, one can creep up on the  $H=1$  condition by adjusting the light source level and the quantizer threshold, starting from a higher light source level (e.g.,  $D \cong 1$ ) and creeping down (i.e., moving from right to left in Fig. 3), while starting from a low quantizer threshold (e.g., also  $D \cong 1$ ) and creeping up. It is noted that the actual quantizer level is likely different from what is set externally due to local circuit variations such as transistor threshold voltage. To sweep the light quanta exposure accurately, a rapidly pulsed light source might be used so that one pulse corresponds perhaps to  $H=0.001$  and 10,000 pulses corresponds to  $H=10$  (keeping the integration time constant). One might adjust an analog voltage on the light source (e.g., LED voltage) to creep down on the  $H=1$  condition.

An example of estimating the read noise and quantizer threshold from  $D - H$  data is illustrated in Fig. 9, where the experimental data comes from [11] and fitted to (8) by adjusting quantizer threshold and input-referred read noise parameters.

In an ensemble of jots, it is expected that due to small circuit variations (e.g., MOSFET threshold voltage variations)

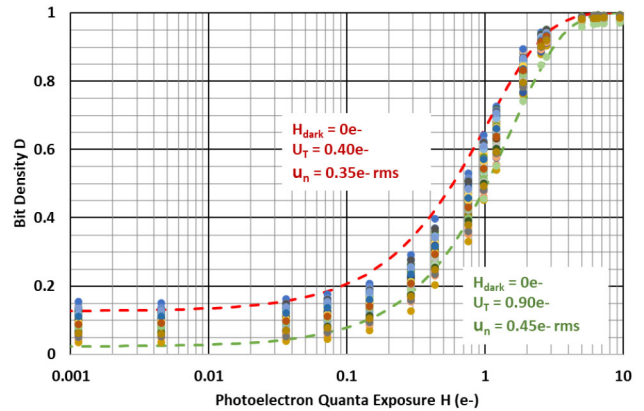


**FIGURE 10.** Experimental 1bQIS density vs. exposure data for 100 randomly selected jots from [11], and model envelopes (dashed lines) calculated using (8).

and read noise variations (e.g., due the  $1/f$  noise variation between source-follower transistors) there will be variation in the  $D - \log H$  characteristics. When measuring an ensemble of jots, the same fitting approach can be used to estimate the envelope of parameters for the ensemble.

An example estimating the envelope parameters is illustrated in Fig. 10 which plots bit density versus exposure from an ensemble of 100 randomly chosen jots, as well as a possible pair of envelope curves calculated using (8). The jot data is the same as that presented in [11]. The parameters were selected to match both the throat spread of the curve ensemble at  $H=1$  and the spread of the curve ensemble at the dark end of the tail ( $H=0.001$ ). The envelopes suggest an estimated spread of quantizer threshold of  $0.50e^-$  and a spread in input-referred read noise of  $0.10e^-$  rms. The fitted read noise for the 1bQIS signal chain data was higher than anticipated since analog readout signal chain PCH measurements using the same jot design yielded about  $0.23e^-$  r.m.s. median [12]. It is hypothesized that more noise is introduced in the 1bQIS quantizer signal chain and further noise reduction may be possible in the future.

### IV. DISCUSSION

Using the 1bQIS bit density model, which depends on input-referred read noise, quantizer threshold and dark current, it is possible to estimate the input-referred read noise of the jot and the quantizer threshold to a surprisingly fine resolution. Small changes in read noise, as low as a few hundredths of an electron r.m.s., and equally small changes to quantizer threshold of a few hundredths of an electron, have an observable effect on the bit density,  $D$ , as a function of quanta exposure,  $H$ . While these parameter estimates that affect fitting have some range in value that could lead to an equally satisfying fit, the magnitude of the fitting freedom is remarkably small. Being able to extract such parameters in the deep sub-electron resolution regime from purely binary output data measurement as a function of exposure is rather interesting and potentially useful in the characterization of quanta image sensors.

## ACKNOWLEDGMENT

The author is grateful to his former and current Ph.D. students for review and discussion of this manuscript. The author also appreciates some fun discussions with Prof. Stanley H. Chan of Purdue University.

## REFERENCES

- [1] E. R. Fossum, "What to do with sub-diffraction-limit (SDL) pixels?—A proposal for a gigapixel digital film sensor (DFS)," in *Program IEEE Workshop Charge-Coupled Devices Adv. Image Sens.*, Karuizawa, Japan, Jun. 2005. [Online]. Available: <https://www.imagesensors.org/Past%20Workshops/2005%20Workshop/2005%20Papers/54%20Fossum.pdf> (Accessed: Mar. 12, 2022).
- [2] E. R. Fossum, J. Ma, S. Masoodian, L. Anzagira, and R. Zizza, "The quanta image sensor: Every photon counts," *Sensors*, vol. 16, no. 8, p. 1260, Aug. 2016, doi: [10.3390/s16081260](https://doi.org/10.3390/s16081260).
- [3] E. R. Fossum, "Modeling the performance of single-bit and multi-bit quanta image sensors," *IEEE J. Electron Devices Soc.*, vol. 1, pp. 166–174, 2013, doi: [10.1109/JEDS.2013.2284054](https://doi.org/10.1109/JEDS.2013.2284054).
- [4] J. Ma, S. Masoodian, D. A. Starkey, and E. R. Fossum, "Photon-number-resolving megapixel image sensor at room temperature without avalanche gain," *OSA Optica*, vol. 4, no. 12, pp. 1474–1481, Dec. 2017, doi: [10.1364/OPTICA.4.001474](https://doi.org/10.1364/OPTICA.4.001474).
- [5] K. Morimoto *et al.*, "Megapixel time-gated SPAD image sensor for 2D and 3D imaging applications," *OSA Optica*, vol. 7, no. 4, pp. 346–354, Apr. 2020, doi: [10.1364/OPTICA.386574](https://doi.org/10.1364/OPTICA.386574).
- [6] K. Morimoto *et al.*, "3.2 megapixel 3D-stacked charge focusing SPAD for low-light imaging and depth sensing," in *Proc. IEEE IEDM*, San Francisco, CA, USA, Dec. 2021, pp. 450–453.
- [7] E. R. Fossum, "Photon counting error rates in single-bit and multi-bit quanta image sensors," *IEEE J. Electron Devices Soc.*, vol. 4, pp. 136–143, 2016, doi: [10.1109/JEDS.2016.2536722](https://doi.org/10.1109/JEDS.2016.2536722).
- [8] D. A. Starkey and E. R. Fossum, "Determining conversion gain and read noise using a photon-counting histogram method for deep sub-electron read noise image sensors," *IEEE J. Electron Devices Soc.*, vol. 4, pp. 129–135, 2016, doi: [10.1109/JEDS.2016.2536719](https://doi.org/10.1109/JEDS.2016.2536719).
- [9] N. A. W. Dutton *et al.*, "Oversampled ITOF imaging techniques using SPAD-based quanta image sensors," in *Proc. Int. Image Sens. Workshop (IISW)*, Vaals, The Netherlands, Jun. 2015, Art. no. 6-04.
- [10] S. H. Chan, private communication, Dec. 2021.
- [11] Z. Yin, J. Ma, S. Masoodian, and E. R. Fossum, "Threshold uniformity improvement in 1b QIS readout circuit," in *Proc. Int. Image Sens. Workshop (IISW)*, Sep. 2021, pp. 214–217.
- [12] J. Ma, private communication, unpublished.



**ERIC R. FOSSUM** (Fellow, IEEE) is the John H. Krehbiel Sr. Professor for Emerging Technologies with the Thayer School of Engineering, Dartmouth College. He is the primary inventor of the CMOS image sensor used in billions of smartphones and other applications and is currently exploring the quanta image sensor. He was awarded the IEEE Andrew Grove Award, the Queen Elizabeth Prize for Engineering in 2017, the OSA/IS&T Land Medal in 2020, and the Technical Emmy Award in 2021, among other honors. He

was the Co-Founder and the First President of the International Image Sensor Society. He was inducted into the National Inventors Hall of Fame and is a Member of the National Academy of Engineering.